

Supergen



Offshore
Renewable
Energy

Early Career Researcher Posters and Abstracts Booklet

2026 Annual Assembly

Surnames M-S



Engineering and
Physical Sciences
Research Council



Early Career Researcher Posters 2026

Charlotte Moss, University of Manchester

Extreme Waves Across Abrupt Depth Transitions

Kasia Patryniak, University of Strathclyde

EnviroClass: environmental conditions clustering for standardisation of FOWTs

Miad Saberi, University of Oxford

Numerical Analysis of Offshore Wind Turbine Monopiles under Partially Drained Conditions

Hibah Saddal, University of Birmingham

Wave-Structure Interaction of Submerged Flexible Plates

Moray Stiven, University of Strathclyde

An investigation into the fatigue crack growth rate in the splash zone region for offshore wind structures

EXTREME WAVES ACROSS ABRUPT DEPTH TRANSITIONS

Charlotte S. Moss¹, David M. Schultz¹, Samuel Draycott², Ben Parkes²

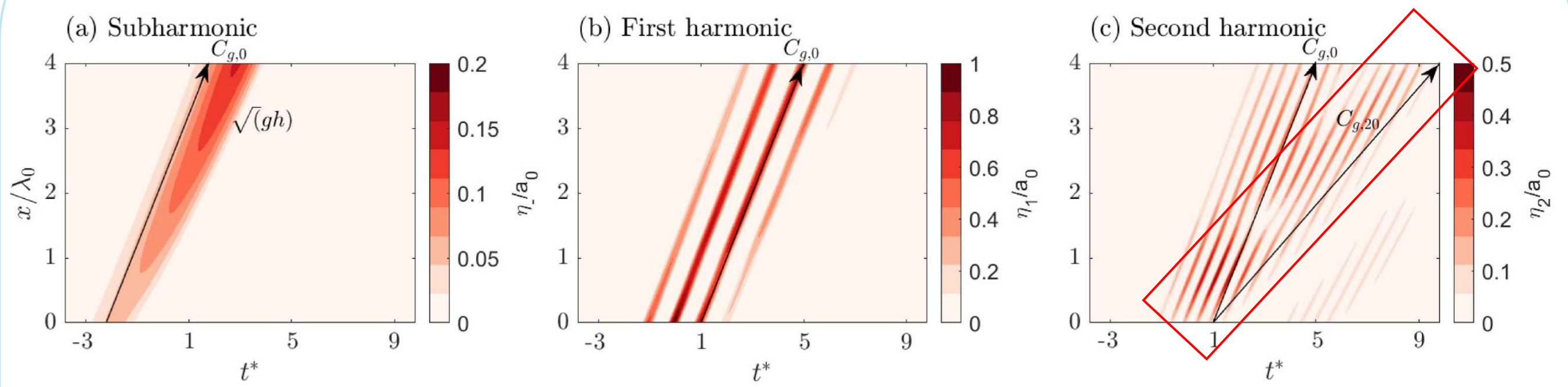
¹School of Natural Sciences, University of Manchester | ²School of Engineering, University of Manchester

Motivation

- Extreme waves have **higher harmonic components** that are often neglected in engineering applications.
- Offshore renewable energy placement usually on **abrupt depth transitions (ADT)**.

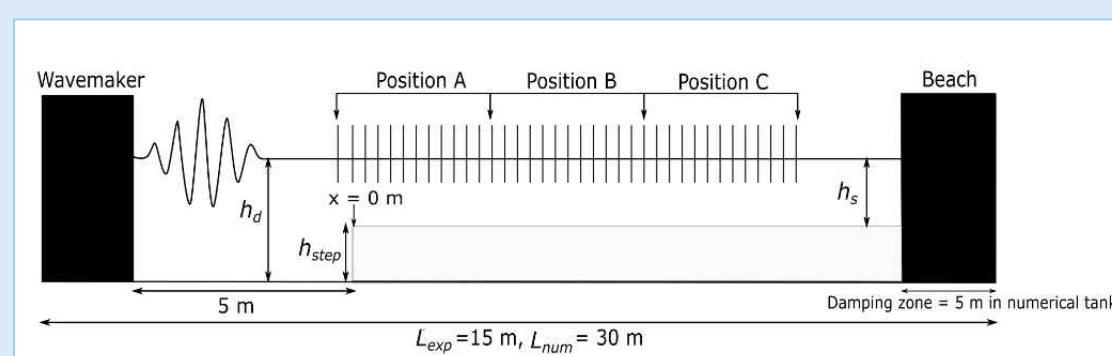
What are we missing?

What happens at an ADT?



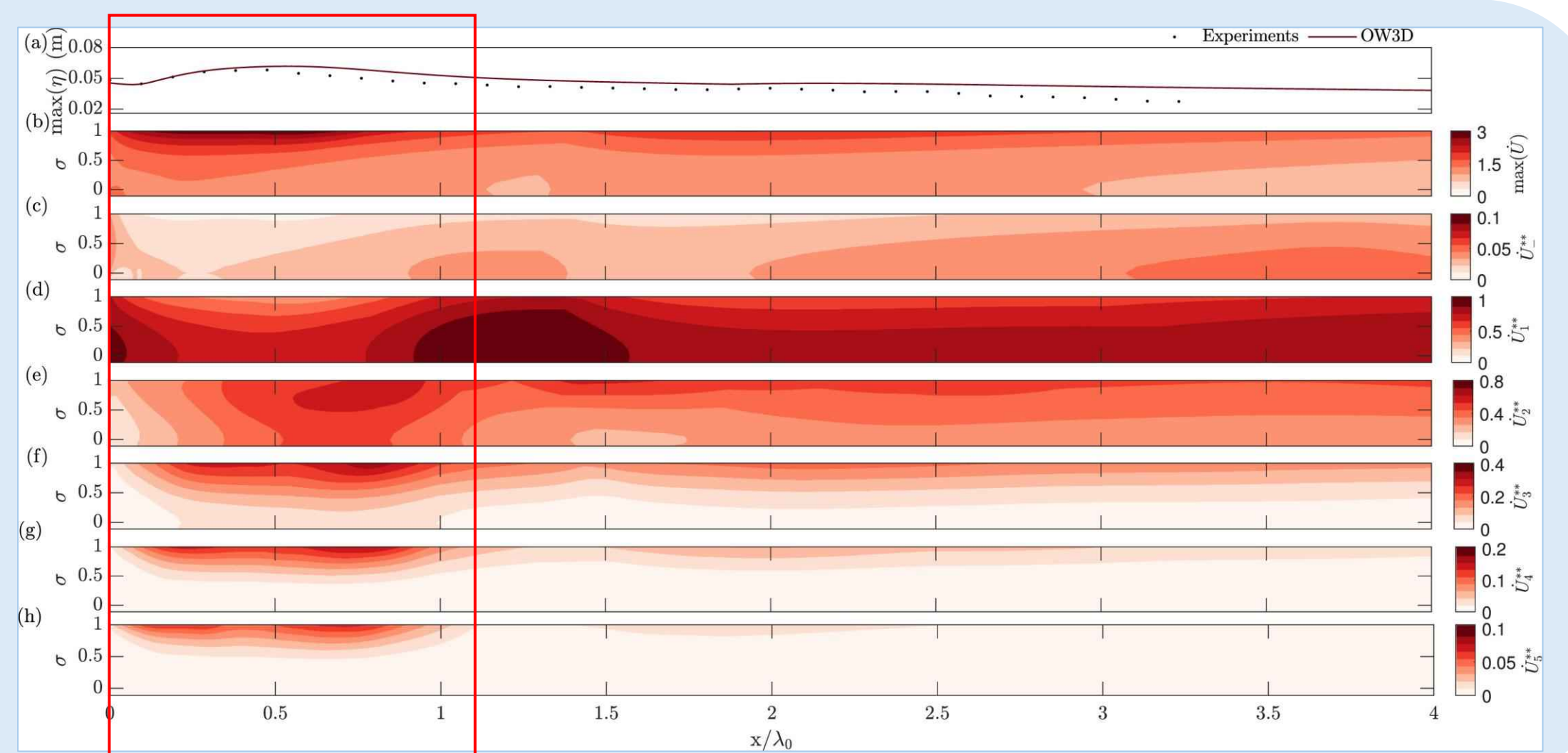
- Two second order free waves are released – one is **transmitted** across the ADT, the other is **reflected**.
- Free and bound components travel at different speeds leading to a **spatial beating pattern**.

1. Step^[1]

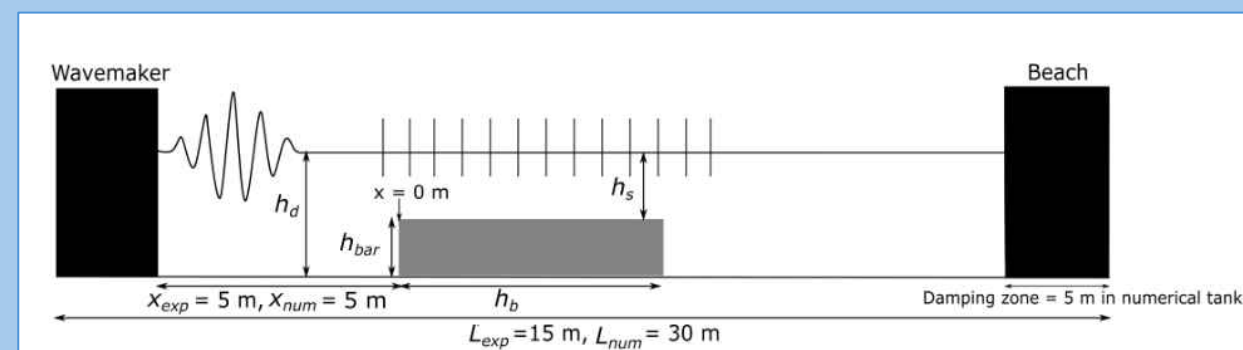


Higher harmonics accounted for:

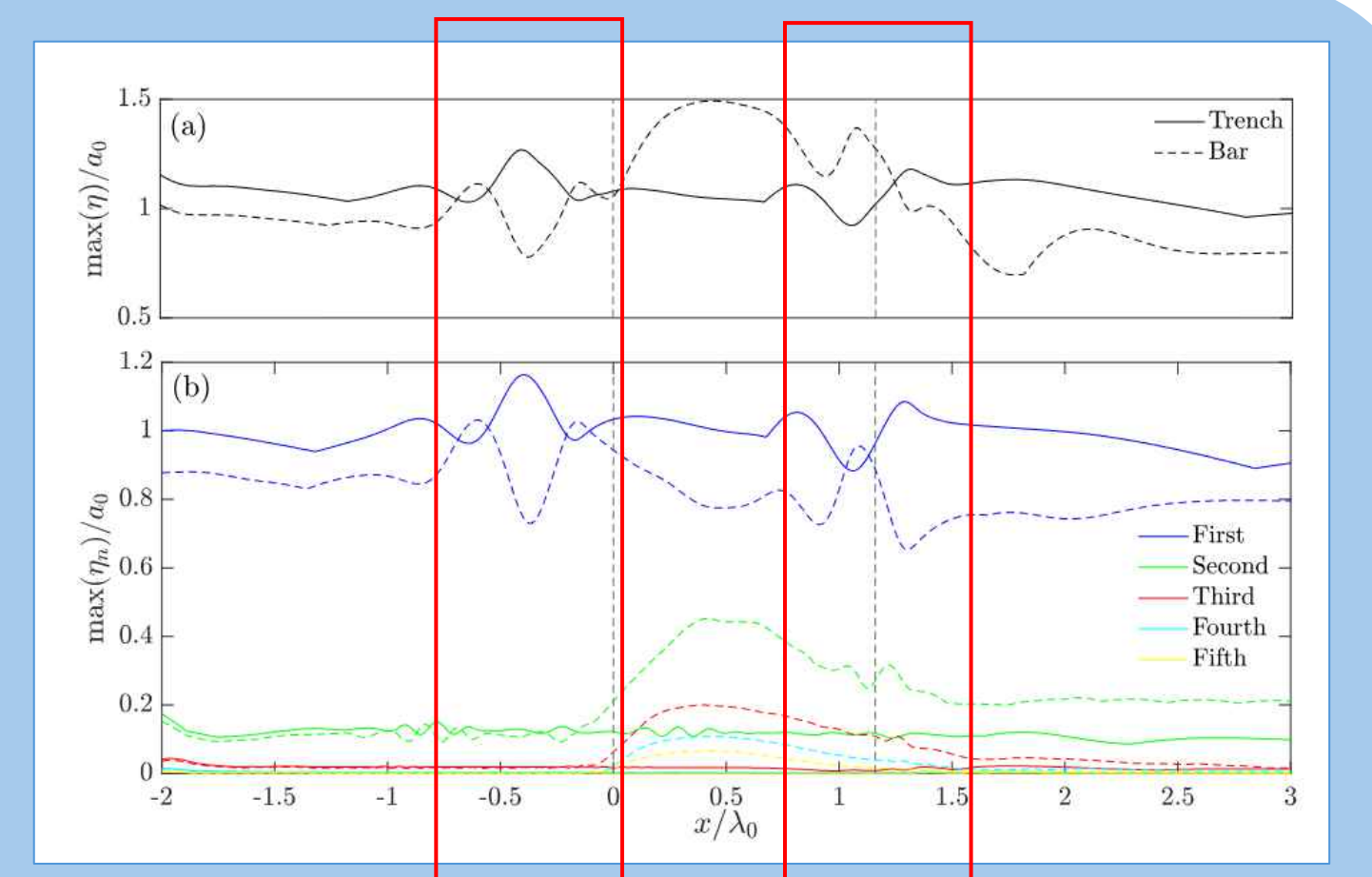
- **25%** of surface elevation
- **30%** of horizontal acceleration
- **33%** of wave force



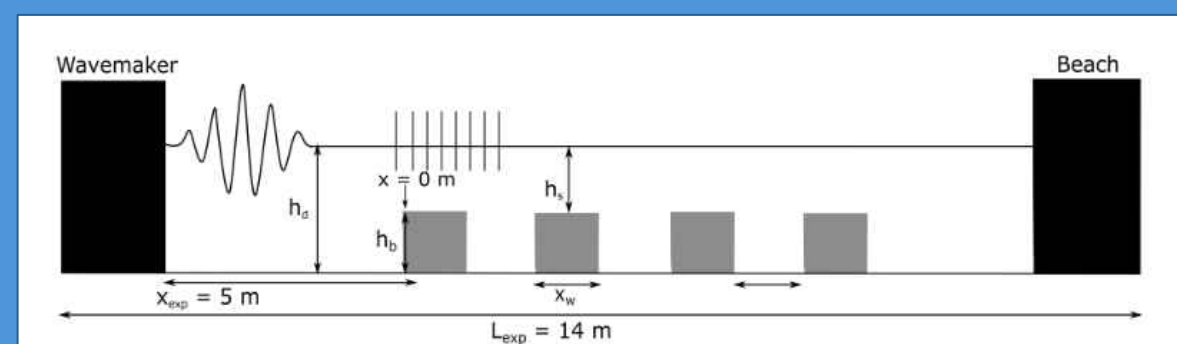
2. Bar and Trench



- Amplitude maxima driven by second harmonic forcing across a bar and linear across a trench.
- Release of an additional **free** second harmonic.

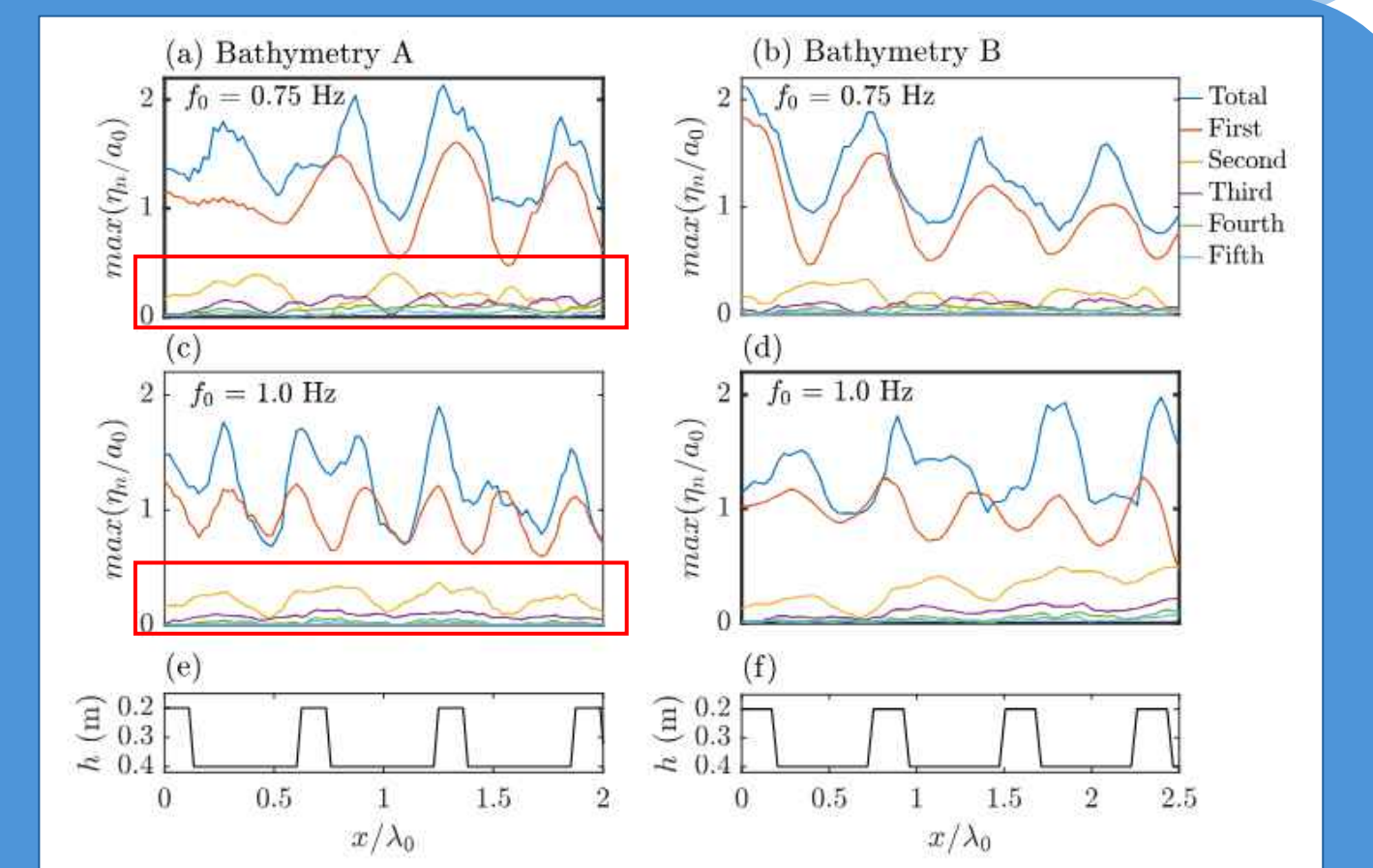


3. Periodic ADTs



'Parasitic beating'

Four wave interactions at the second harmonic between the free and bound, transmitted and reflected wave components.



Implications

- Results demonstrate higher-harmonics and free-bound interactions are an important consideration for waves across an ADT.
- Findings can be applied to offshore renewable energy system design/placement and design methods, maritime safety, and coastal protection.

References



[1] Moss, C.S., Schultz, D.M., Parkes, B., Li, Y. and Draycott, S., 2025. Higher-harmonic contributions to surface elevation, kinematics, and wave loads in wave packets across an abrupt depth transition. *Coastal Engineering*, 197, p.104693.

EnviroClass: environmental conditions clustering for standardisation of FOWTs

Kasia Patryniak¹, Maurizio Collu¹, Ajit Pillai²

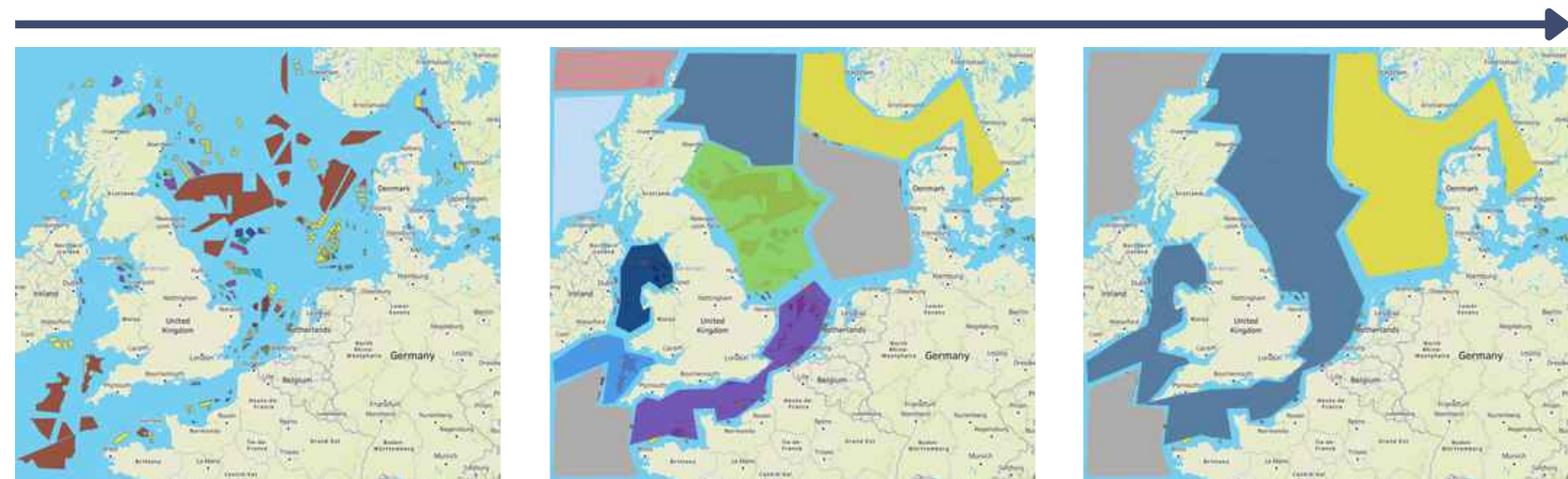
¹University of Strathclyde, ²University of Exeter, Supported by: SSE, Scottish Power, Stiesdal Offshore, Floatation Energy, JMU, DNV, and LR



01. Aim

The central trade-off in design standardisation is determining the optimum number of offshore zones.

Standardisation = benefits of scale



Bespoke optimisation = less overengineering

- **Single global zone** → Universal design for the severest conditions, over-engineered for most locations
- **Small zones** → Site-specific optimisation, no economies of scale
- **"Sweet spot"** → Minimum total cost, fast delivery, reliability



02. Introduction

Do we really need a bespoke floating offshore wind turbine for every site?

It's 2040. A floating wind developer has just secured a new lease off the coast of Scotland. Within days, the team knows which support structure to propose as the concept design, complete with a CAPEX estimate.

They can do this because the floating wind platform provider's portfolio already includes five standardised designs, each matched to a different "sea type", and they identified the sea type the developer's site belongs to.

These sea types aren't arbitrary — they're derived from data-driven clustering of a long-term metocean dataset.

Instead of starting from scratch, the developer selects the best-fit design, confident it's technically feasible and cost-competitive. The project moves forward at speed, while economies of scale from standardisation keep costs down.

Of course, site-specific optimisation still happens after the award, but the heavy lifting has already been done. Developers go into leasing rounds with clarity and confidence, and the industry as a whole benefits.

That's the **vision**. The EnviroClass project is a step toward making it a reality.

03. Methodology

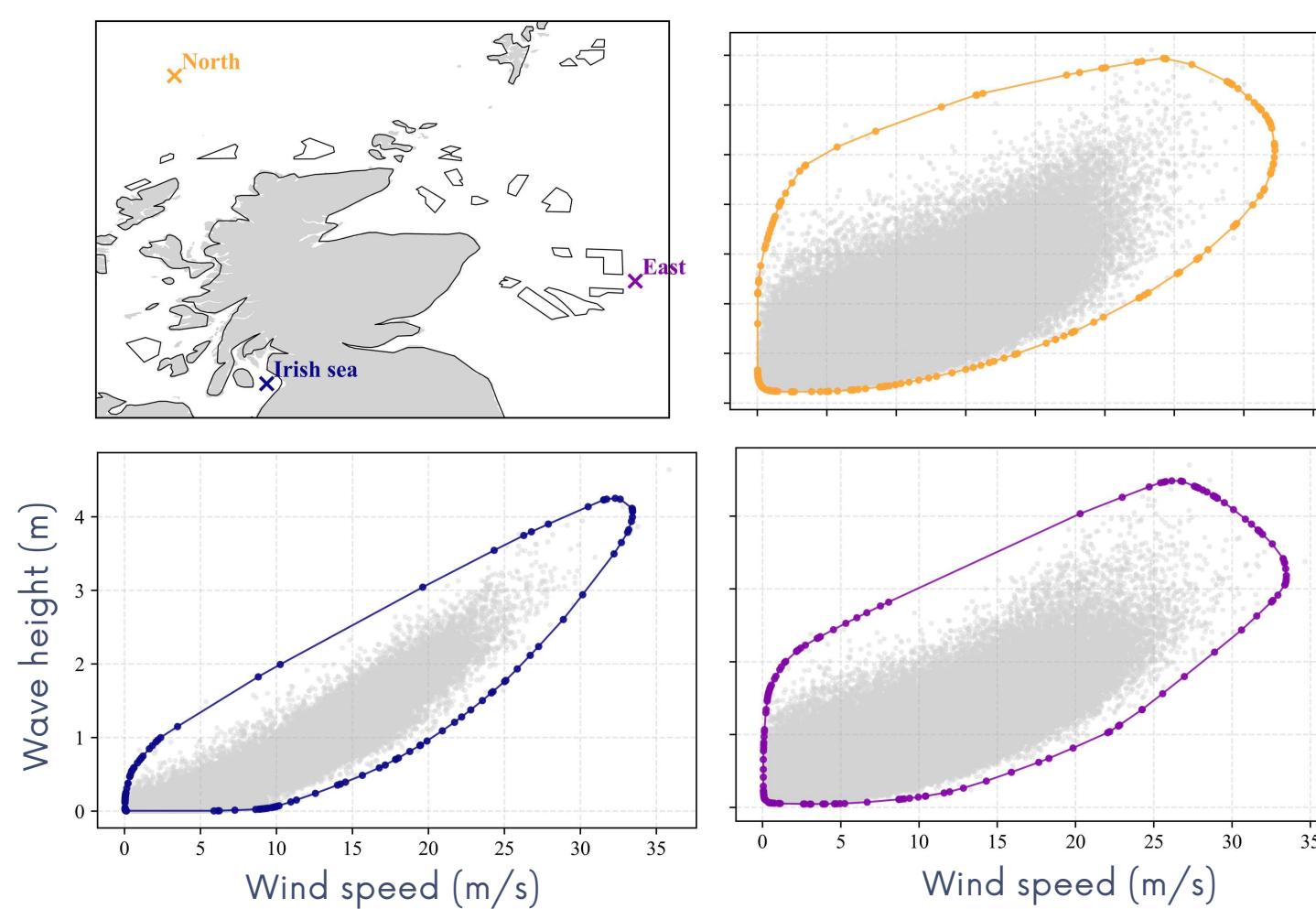
The "EnviroClass" approach is designed around 6 steps:

1. Design-driving load cases and environmental parameters — to ensure direct relevance to structural design.

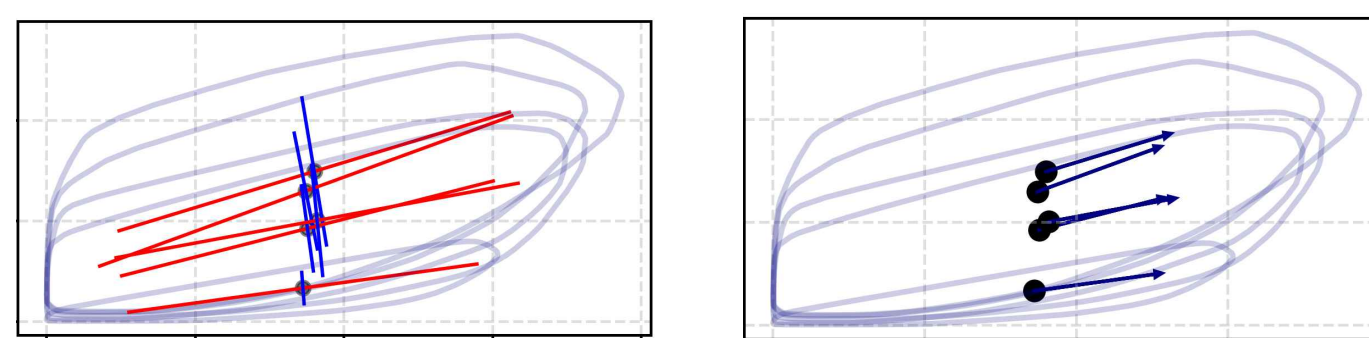
DLC 1.6, 6.1 → 50-year return period contours, misalignment

2. Extreme value analysis — methods are adapted for consistent, automated computation across large spatial domains.

POT + Generalised Pareto Distribution + Direct IFORM

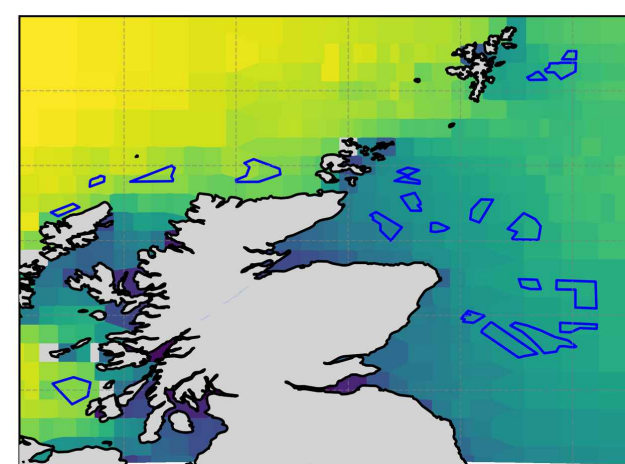
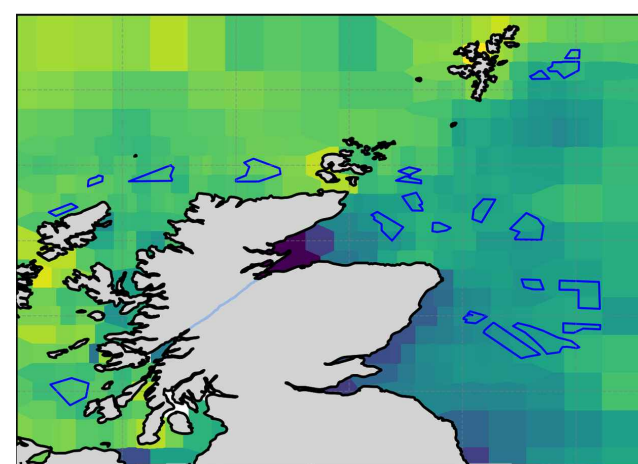


3. Feature extraction: (PCA) Scalar features extracted from the environmental contours: area, orientation, major & minor axes, aspect ratio, centroid, max(Hs), max(UV):

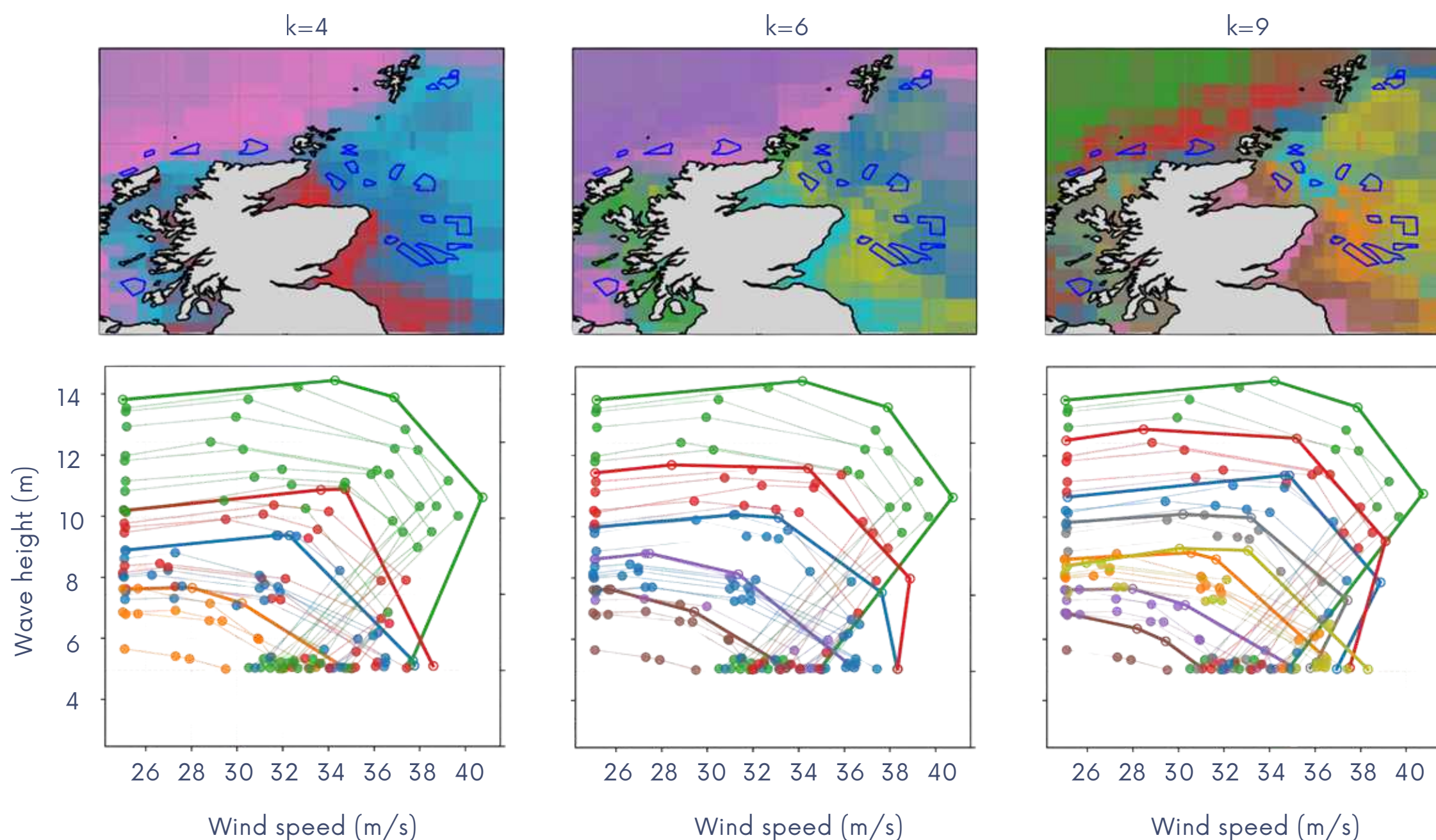


Centroid x

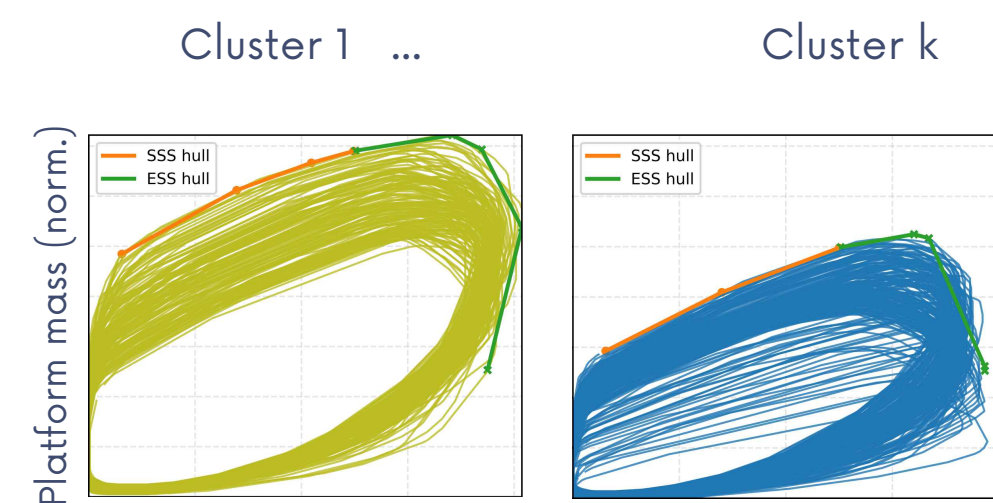
max(Hs)



4. C-means clustering — unbiased, multi-parameter grouping of environmental conditions, avoiding the subjective zone boundaries



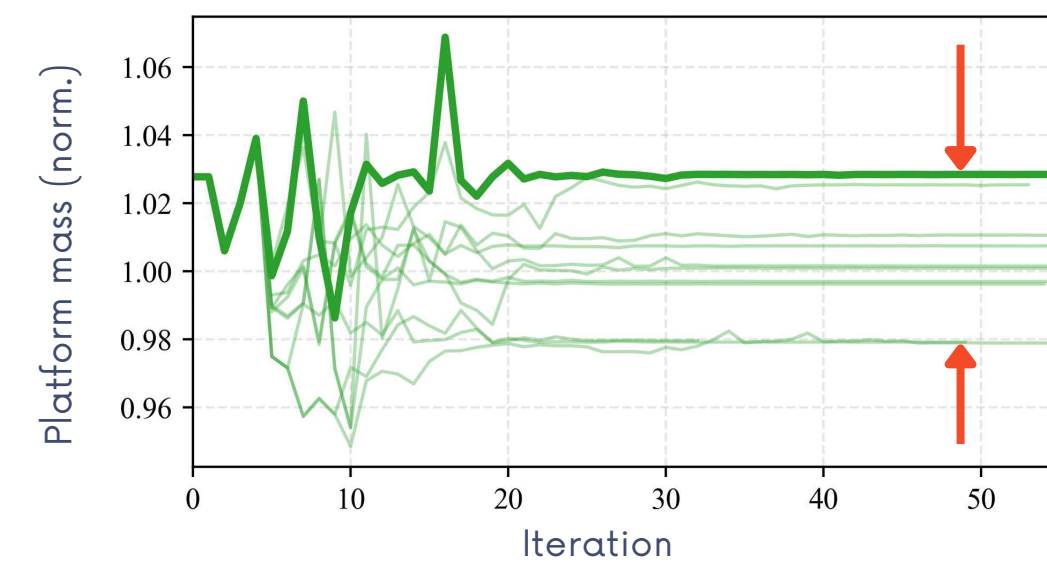
5. "Super-contours" — cluster-representative environmental conditions



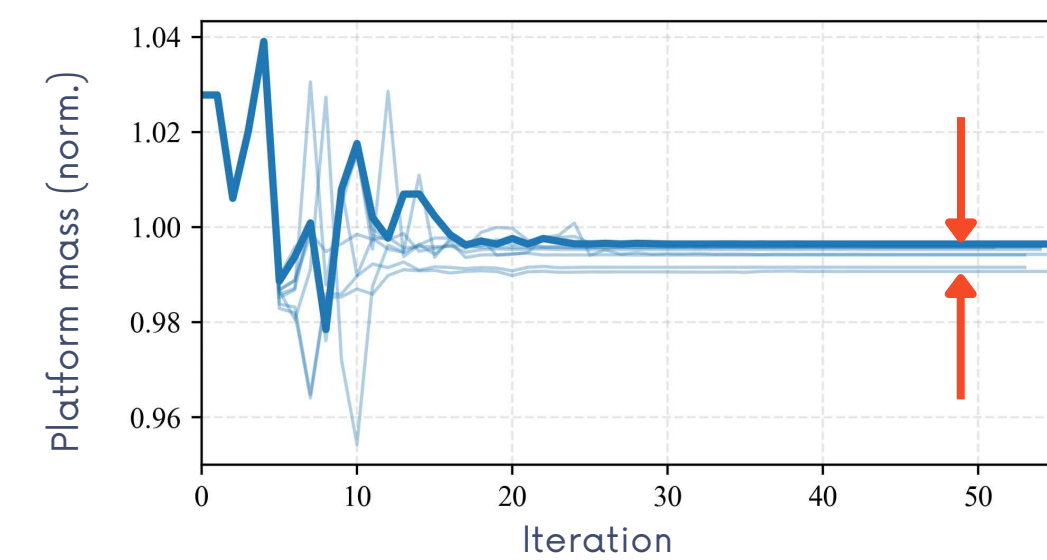
6. Application — standardised platform design/optimisation (WEIS):

- Thick history: design per cluster
- Thin history: design per site

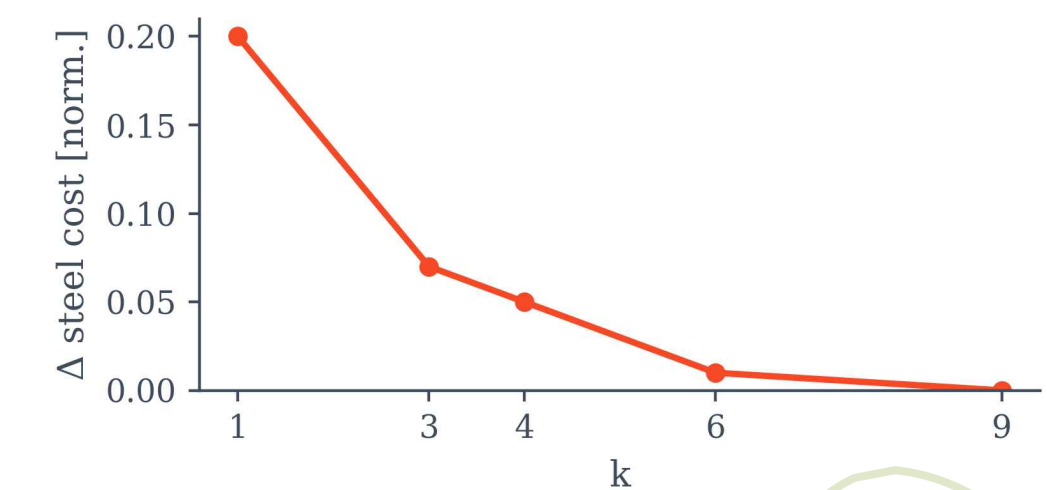
3 zones clustering experiment, zone 2:



6 zones clustering experiment, zone 3:



Overengineering curve: how much heavier the standardised platforms are on average for a given number of clusters:



Your comments

Numerical Analysis of Offshore Wind Turbine Monopiles under Partially Drained Conditions

Miad Saberi, Guy T. Houlsby, Luc E. J. Simonin, Byron Byrne
 Department of Engineering Science, University of Oxford, UK
 *Email: miad.saberi @eng.ox.ac.uk



UNIVERSITY OF
OXFORD

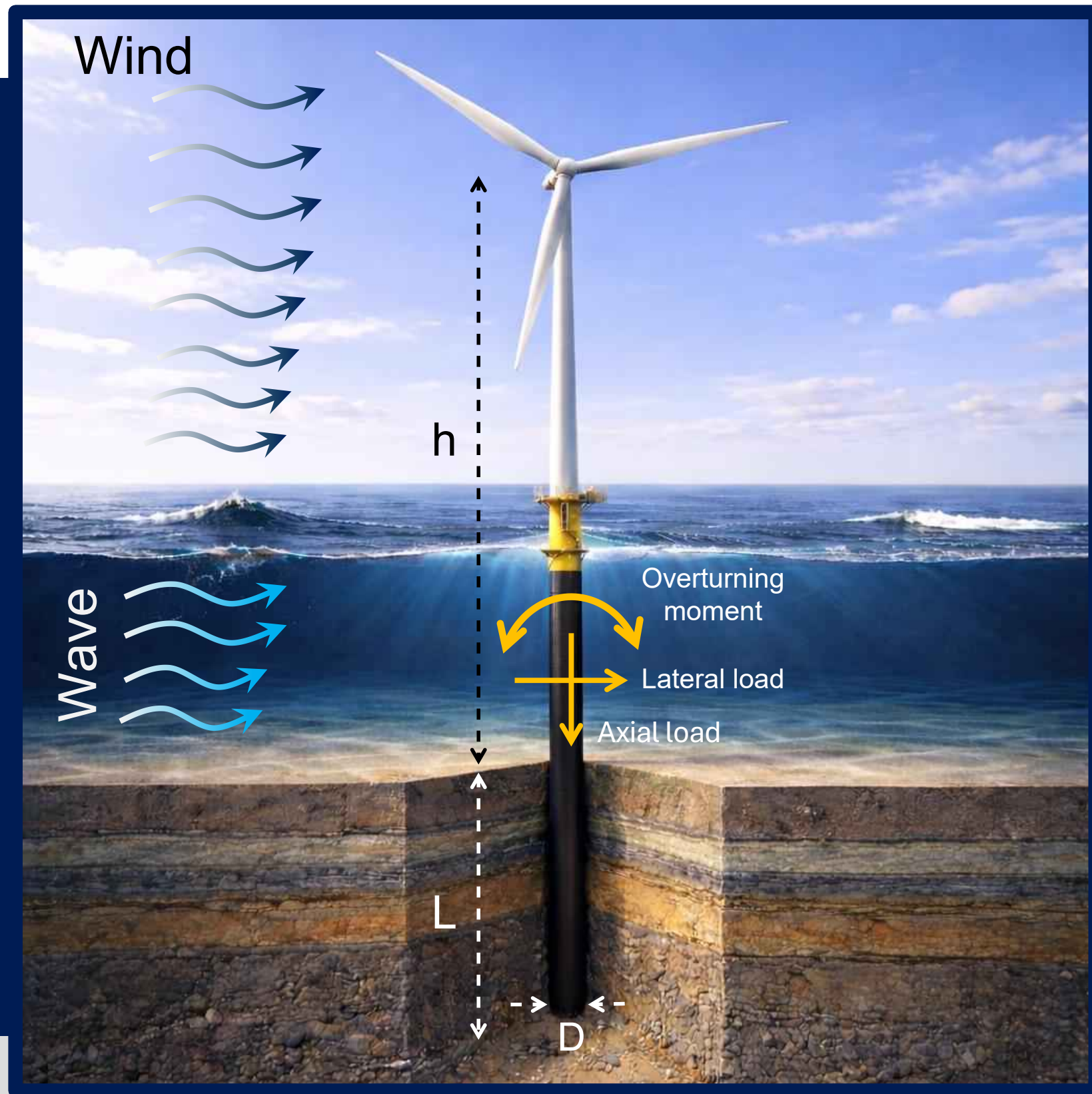


Fig.1 Monopile foundation for OWT

Introduction

The behaviour of monopile foundations for offshore wind turbines (OWTs), which are large-diameter steel piles with L/D ratios of about 3 to 8, is strongly influenced by **loading rate under partially drained conditions**.

In saturated sand, loading may develop either positive or negative excess pore water pressures, depending on the sand relative density, leading to a decrease or increase in effective stress and consequently changes to the pile capacity.

This study investigates the response of medium-scale monopiles in sand across a wide range of loading rates, from drained to partially drained and undrained conditions, using three-dimensional (3D) finite element (FE) analyses with the advanced hyperplasticity-based HySand constitutive model.

Sands ranging from loose to very dense were analysed, and monopile capacity under different drainage conditions was predicted.

HySand Constitutive Model

HySand is a hyperplasticity-based effective stress model, founded on thermodynamic principles and formulated with multiple yield surfaces (Simonin 2023; Simonin *et al.* 2026).

Gibbs energy function (g):

$$g = -\frac{p_r}{k_r(1-m)(2-m)} \left(\frac{p_0}{p_r}\right)^{2-m} - \frac{1}{N} \sigma_{ij} \sum_{n=1}^N \alpha_{ij}^{(n)} - \frac{1}{N} \frac{I_{1\sigma}}{3} \sum_{n=1}^N \alpha_{pc}^{(n)}$$

$$p_0^2 = \frac{\sigma_{ii}\sigma_{jj}}{9} + \frac{k_r(1-m)}{2g_r} \sigma'_{ij}\sigma'_{ij}$$

Yield functions (y):

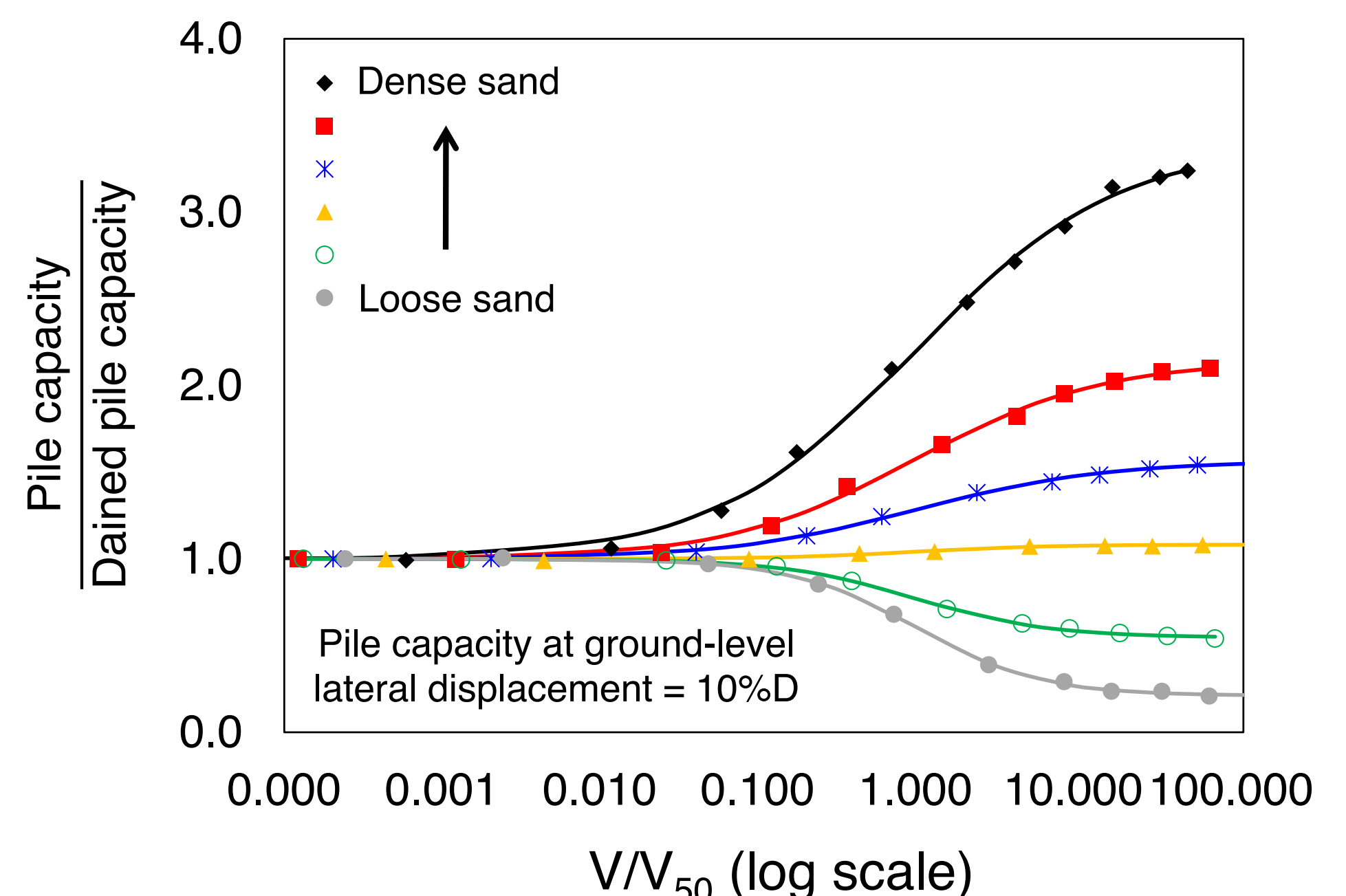
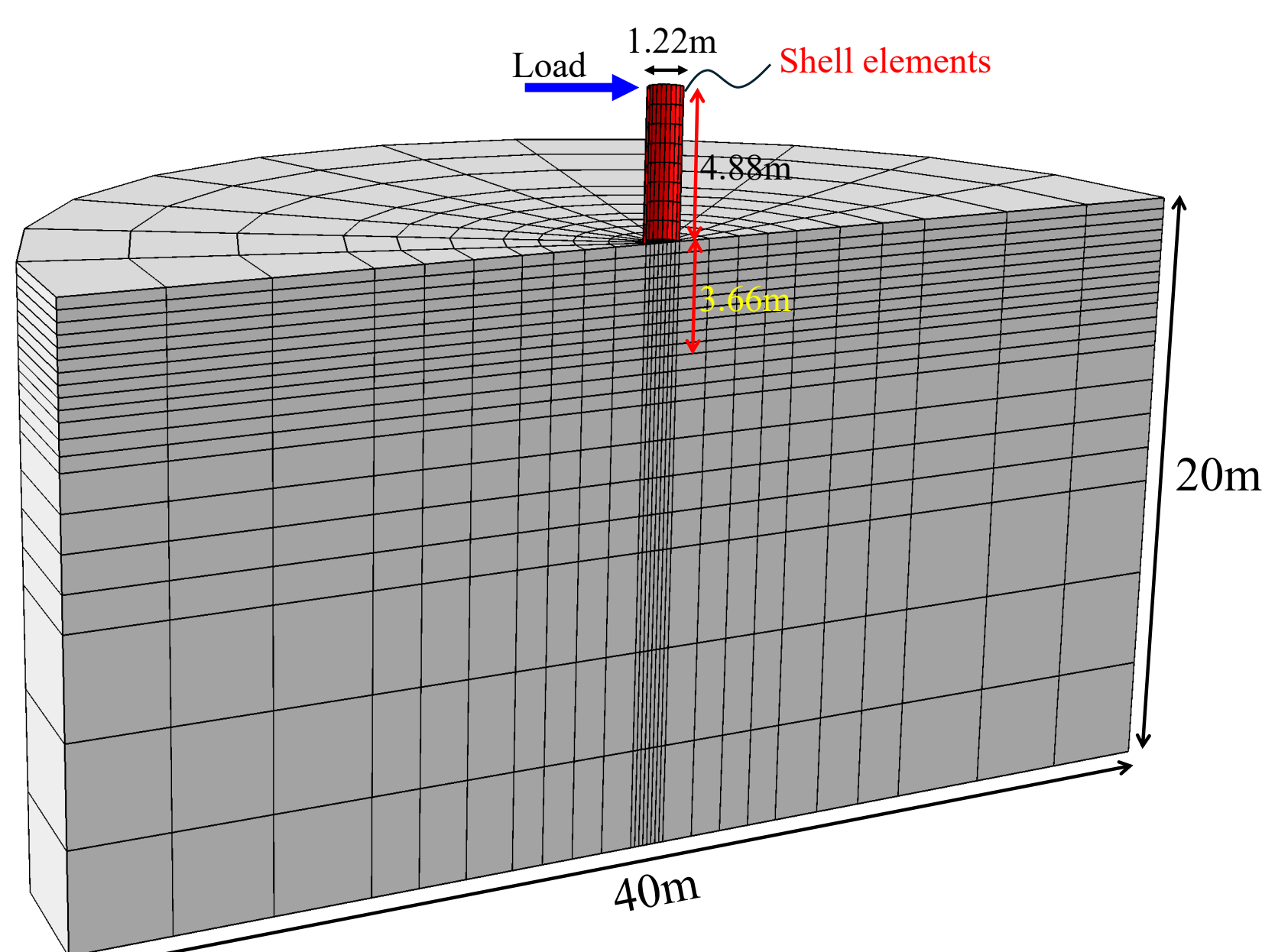
$$y^{(n)} = \frac{4I_{1\sigma}J_{2X}^{(n)} - 3tr(\sigma X^{(n)2})}{8\left(\frac{n}{N}\mu\right)^2 I_{3\sigma}} + \left(\frac{N\chi_{pc}^{(n)}}{p_c^{(n)}}\right)^r - 1$$

$$\chi_{ij}^{(n)} = N\chi_{ij}^{(n)'} - h_n(\alpha_{ij}^{(n)}, \sigma) - \sqrt{\frac{2}{3}} a_{ij} \beta^{(n)} \frac{N\chi_{kk}^{(n)}}{3} + \sqrt{\frac{2}{3}} A(1 - \sqrt{2J_{2a}}) x'_a$$

Model parameters:

Elastic bulk stiffness	k_r	Max. specific volume	B	Max. anisotropy rate factor	A_{max}
Elastic shear stiffness	g_r	Critical state specific volume	Γ	Max. hardening factor	h_0
Stiffness exponent	m	Min. specific volume	Δ	Hardening factor exponent	b
Critical state stress ratio	μ	Critical state line slope	λ_B	Consolidation exponent	r
Max. dilation rate	β_{max}	Consolidation line slope at max. Density	λ_Δ		

FE Model & Numerical Predictions



References:

- Simonin, L. (2023). Development of an effective stress model for sand under cyclic loading in the hyperplastic framework. DPhil thesis, University of Oxford, UK.
- Simonin, L., Houlsby, G. and Byrne, B. (2026), "The HySand hyperplasticity constitutive model for sand: theory", *Géotechnique*.

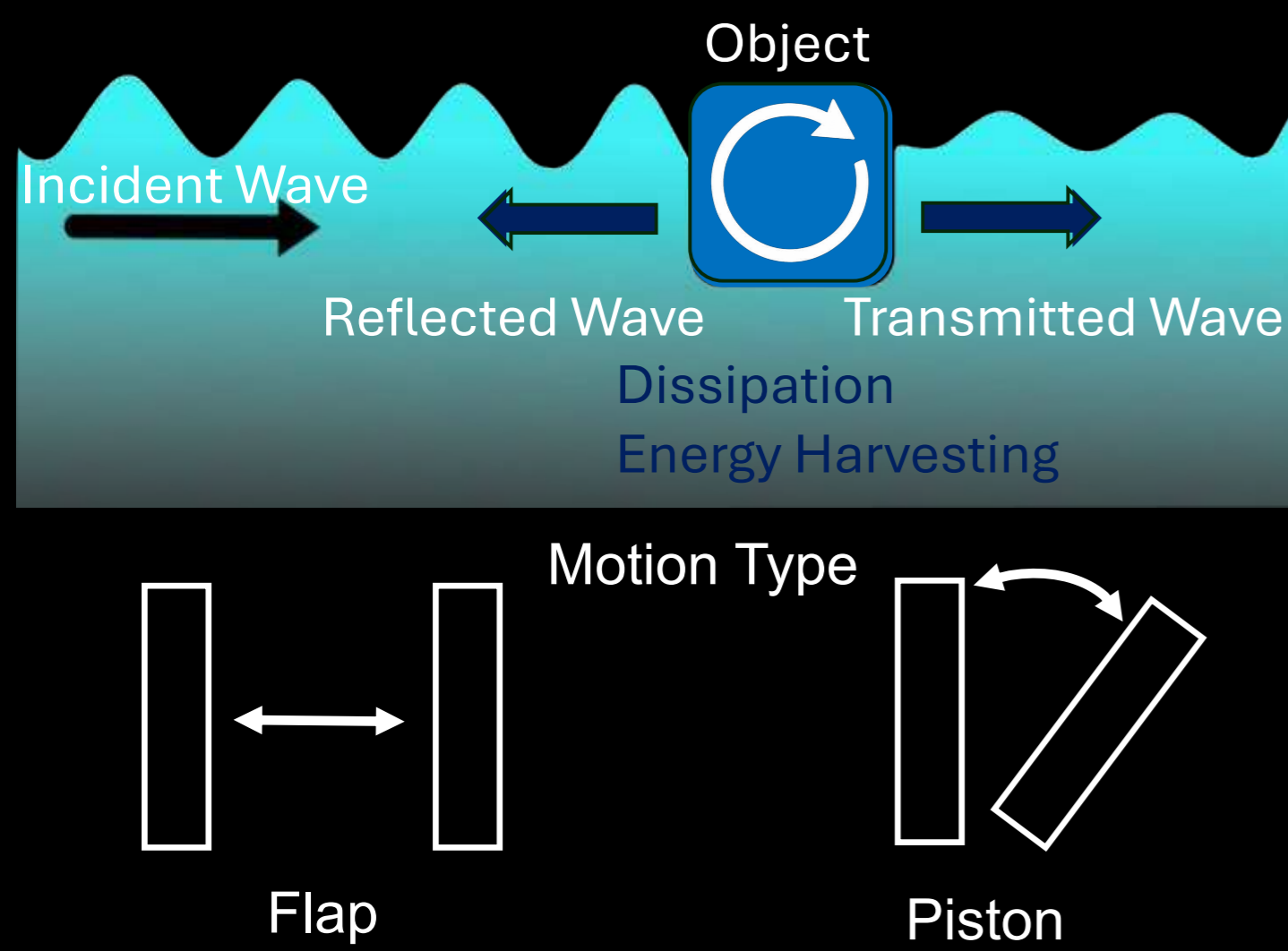
Wave-Structure Interaction of Submerged Flexible Plates

Hibah Saddal¹, Gatien Polly², Diane Komaroff², Benjamin Thiria², Ramiro Godoy-Diana², Chandan Bose¹

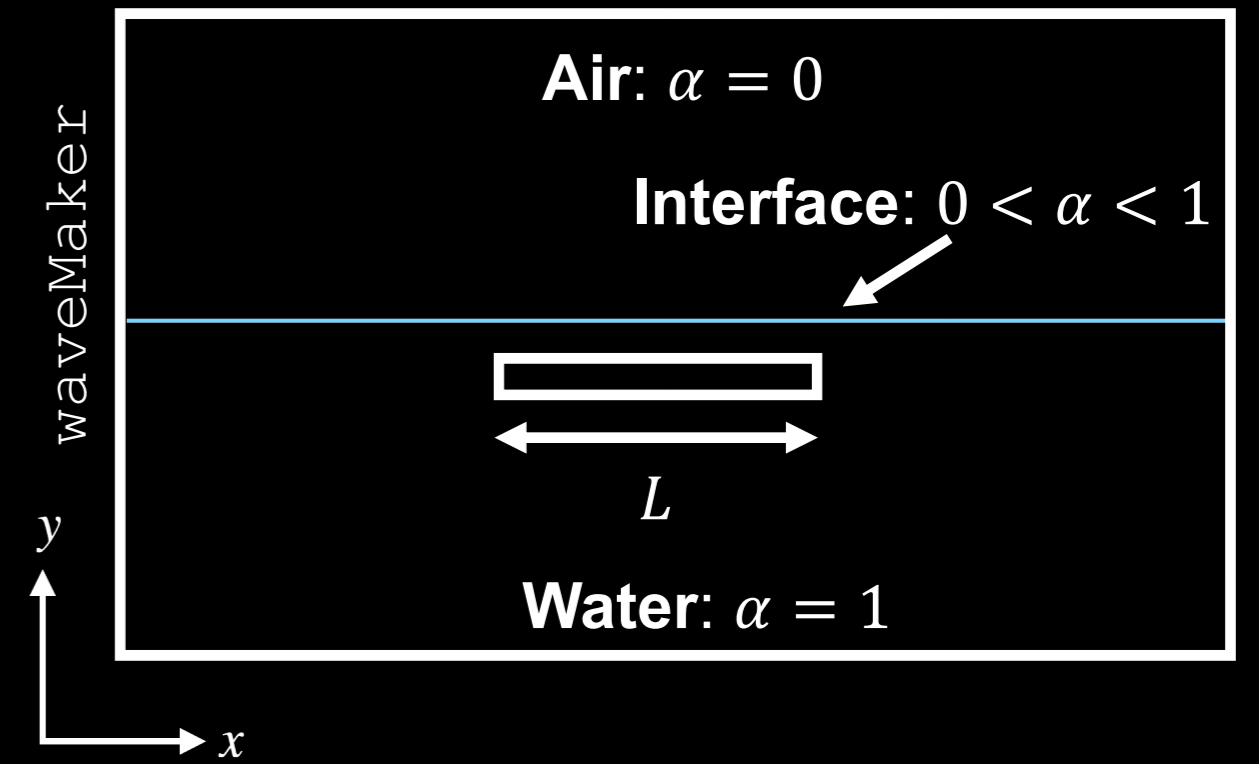
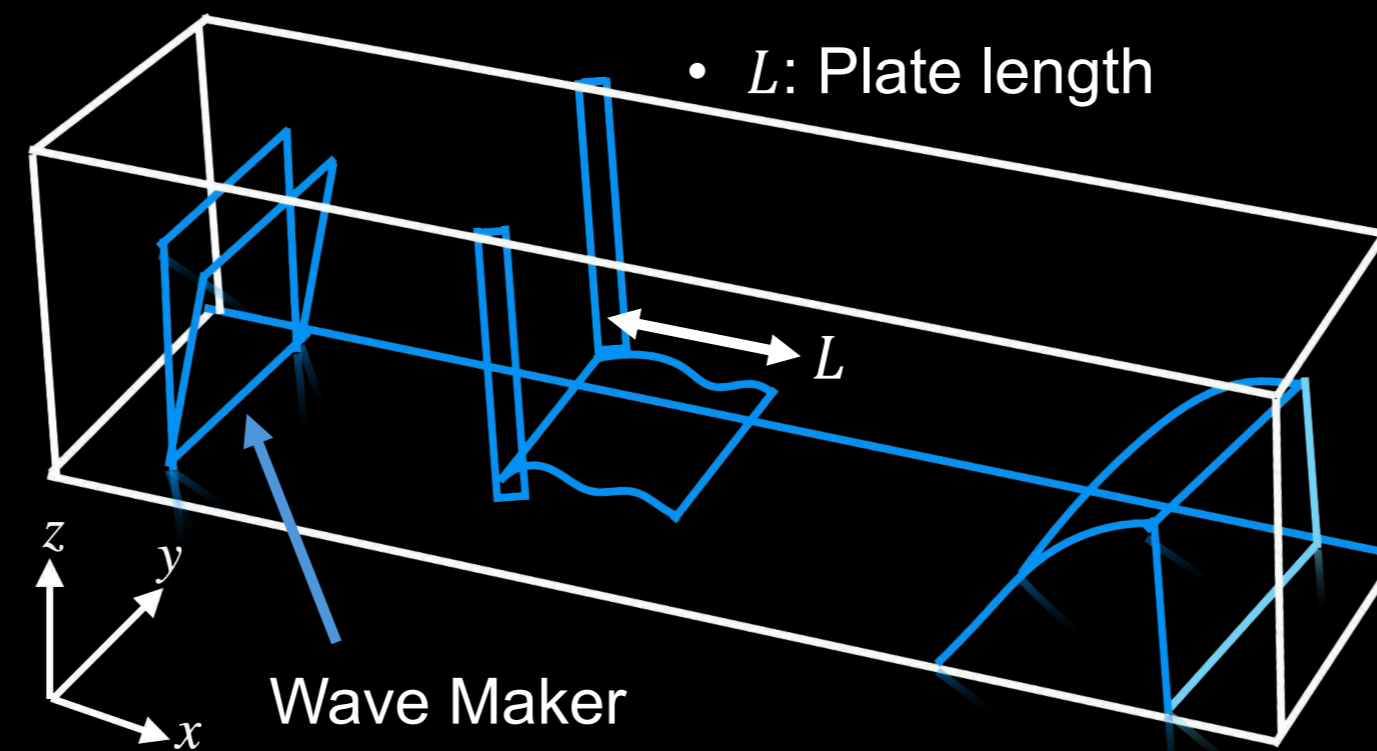
¹Bioinspired Fluid-Structure Interaction Laboratory, Aerospace Engineering, School of Metallurgy and Materials, University of Birmingham

²Laboratoire de Physique et Mécanique des Milieux Hétérogènes (PMMH), CNRS UMR 7636, ESPCI Paris-Université PSL, Sorbonne Université, Université Paris Cité

Email: c.bose@bham.ac.uk



A submerged flexible plate can reflect, transmit, and significantly attenuate water waves, depending on wave conditions and structural properties. Its hydroelastic response plays a crucial role in dissipating wave energy under certain conditions, thereby making such systems promising for sustainable wave energy conversion applications.



The two-phase incompressible Navier-Stokes equations in the Arbitrary Lagrangian Eulerian formulation.

$$\nabla \cdot \mathbf{u} = 0$$

$$\frac{\partial \mathbf{u}}{\partial t} + [(\mathbf{u} - \mathbf{u}^m) \cdot \nabla] \mathbf{u} = -\frac{1}{\rho_f} \nabla p + \nu \nabla^2 \mathbf{u} + \mathbf{g} + \frac{1}{\rho_f} \mathbf{F}_\sigma$$

Volume of Fluid method, α is the phase indicator variable:

$$\rho_f = \alpha \rho_{\text{water}} + (1 - \alpha) \rho_{\text{air}}$$

$$\mathbf{v} = \alpha \mathbf{v}_{\text{water}} + (1 - \alpha) \mathbf{v}_{\text{air}}$$

$\alpha = 1$: water
 $\alpha = 0$: air
 $0 < \alpha < 1$: interface

- \mathbf{u} : Fluid velocity
- \mathbf{u}^m : Grid point velocity
- ρ_f : Fluid density
- p : Fluid pressure
- ν : Kinematic viscosity
- \mathbf{g} : Gravitational acceleration
- \mathbf{F}_σ : Surface tension

The hyper-elastic structure is governed by the Neo-Hookean model; The strain-energy density function W is given by:

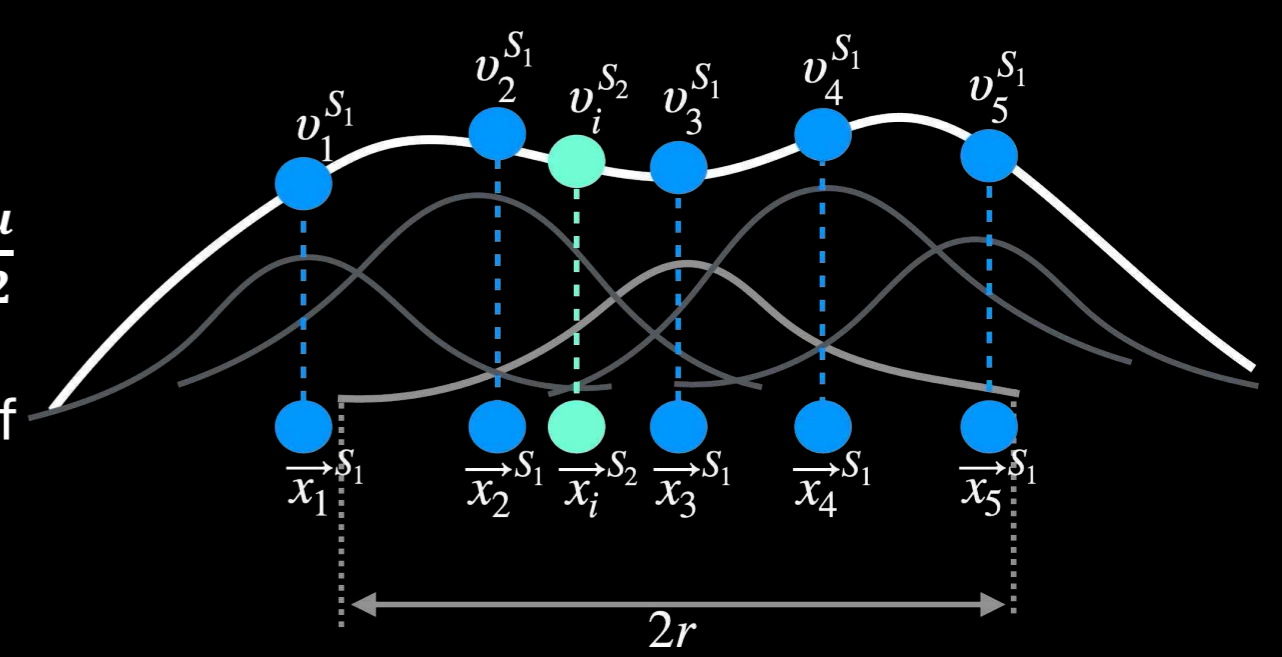
$$W = C_{10}(\bar{I}_1 - 3) + \frac{1}{D_1}(J - 1)^2,$$

\bar{I}_1 is the first invariant of the deviatoric part of the right Cauchy-Green deformation tensor
 J is the determinant of the deformation gradient

$$D_1 = \frac{2}{\lambda}$$

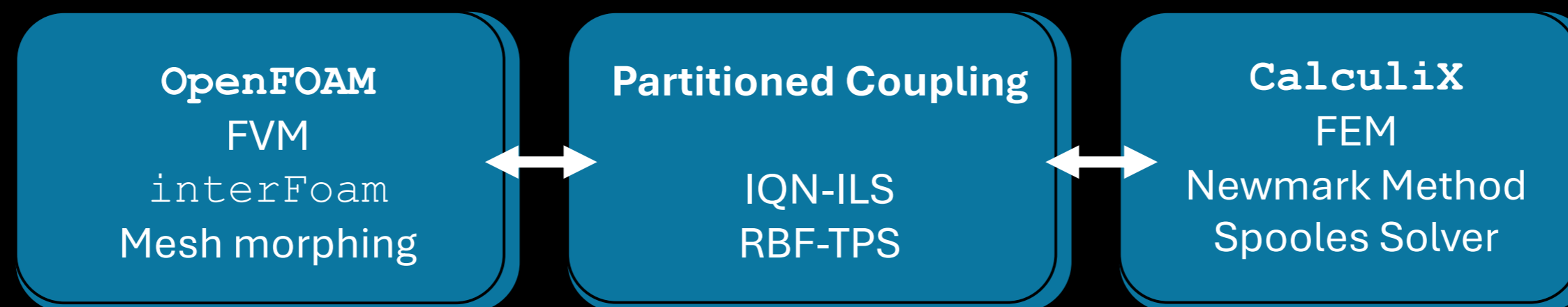
$$C_{10} = \frac{\mu}{2}$$

Date Mapping Scheme at the Fluid-Structure Interface: Radial-Basis Function Interpolation

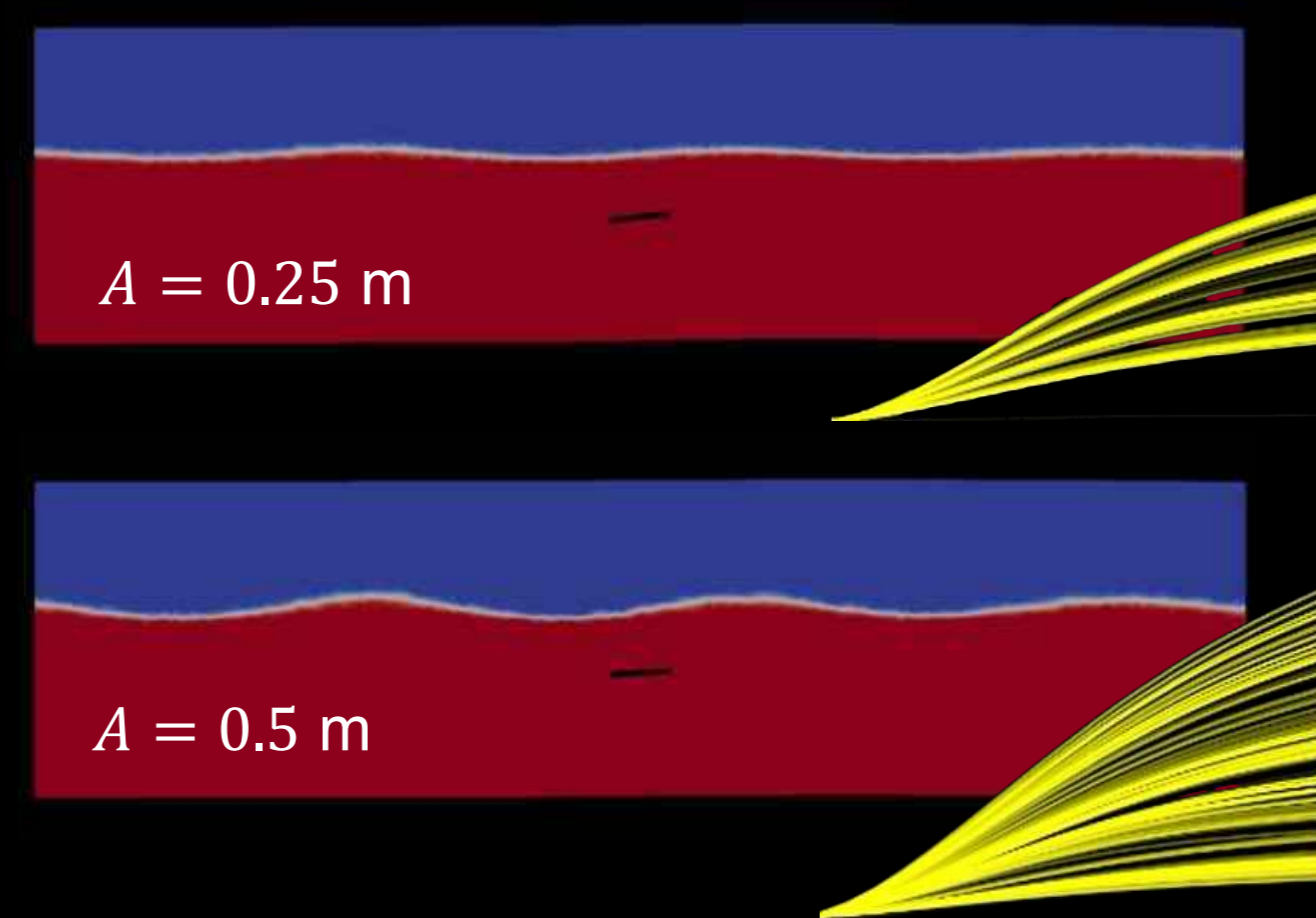
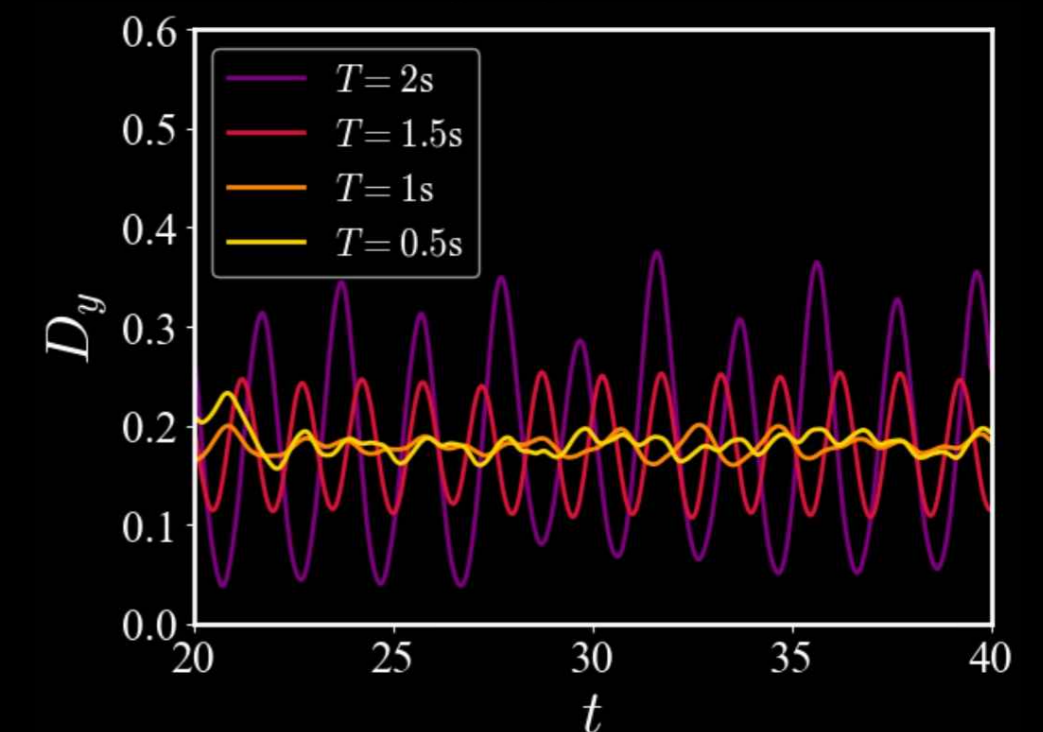
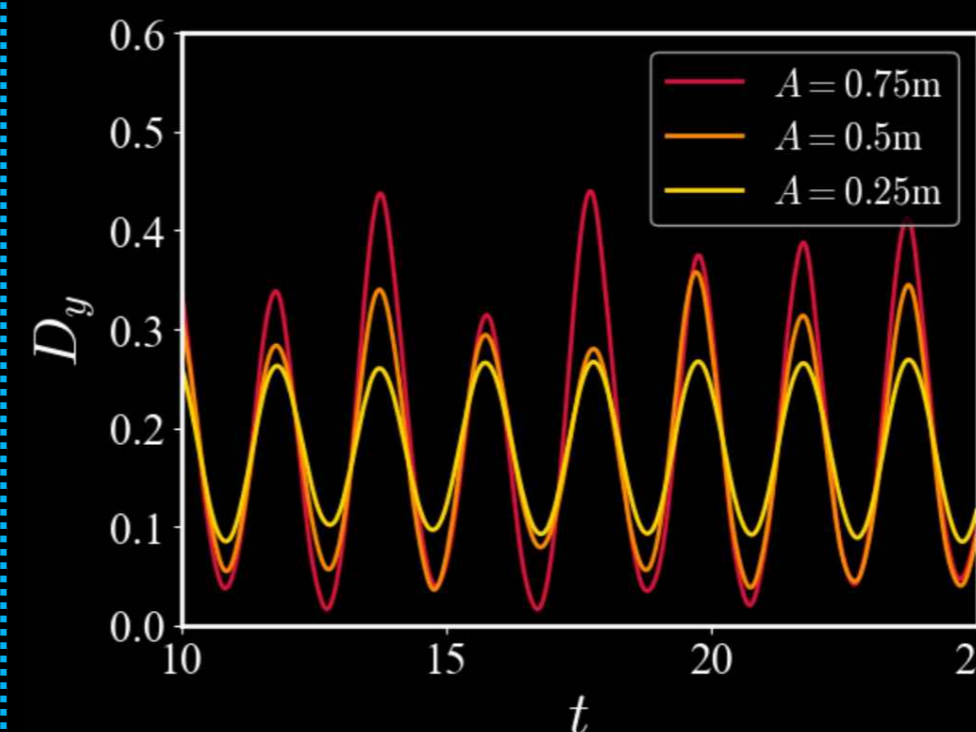
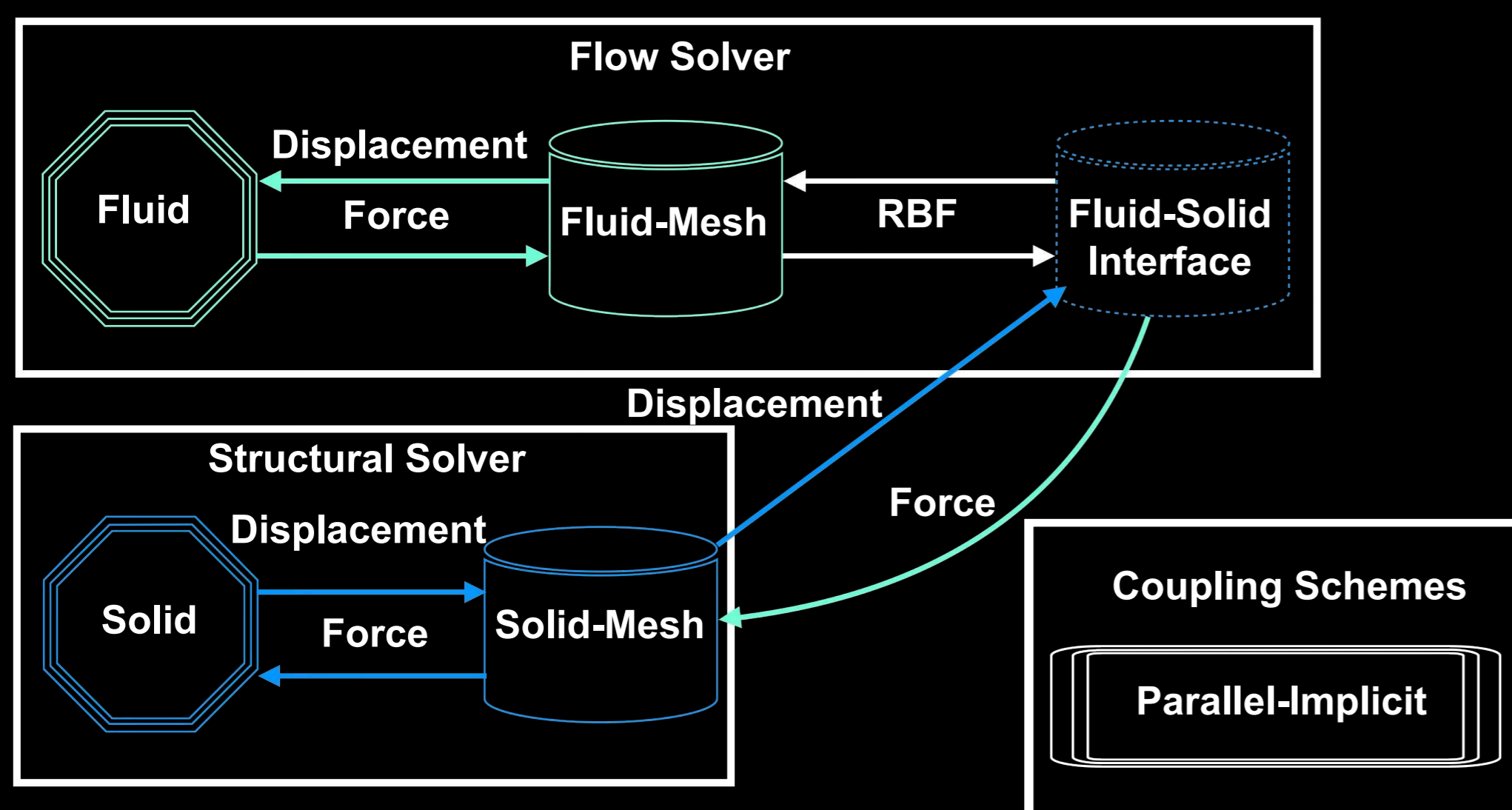


$$f_{\text{recv}}(x) = \sum_{i=1}^N \gamma_i \phi(\|x - x_i\|)$$

ϕ is the radial basis function and γ_i are coefficients determined from the known values at points x_i .

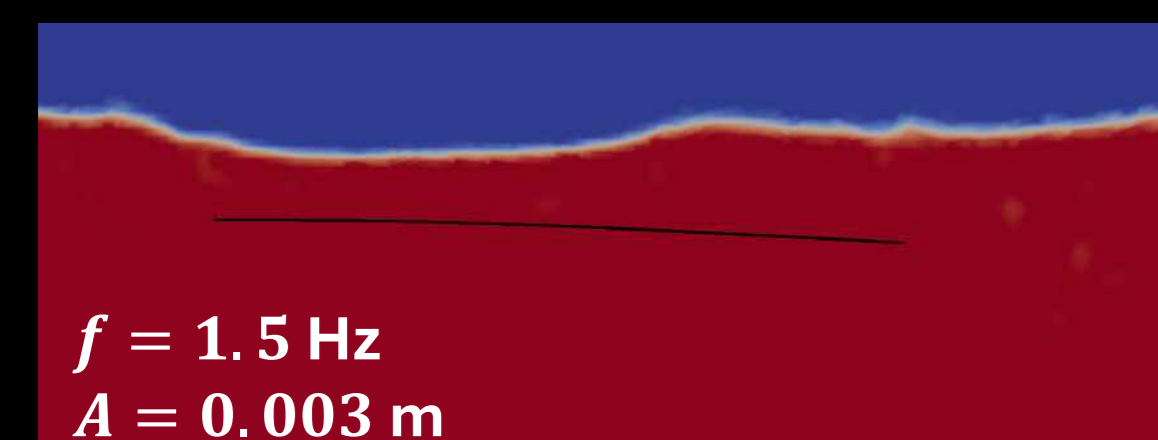


Fluid-Structure Coupling Workflow

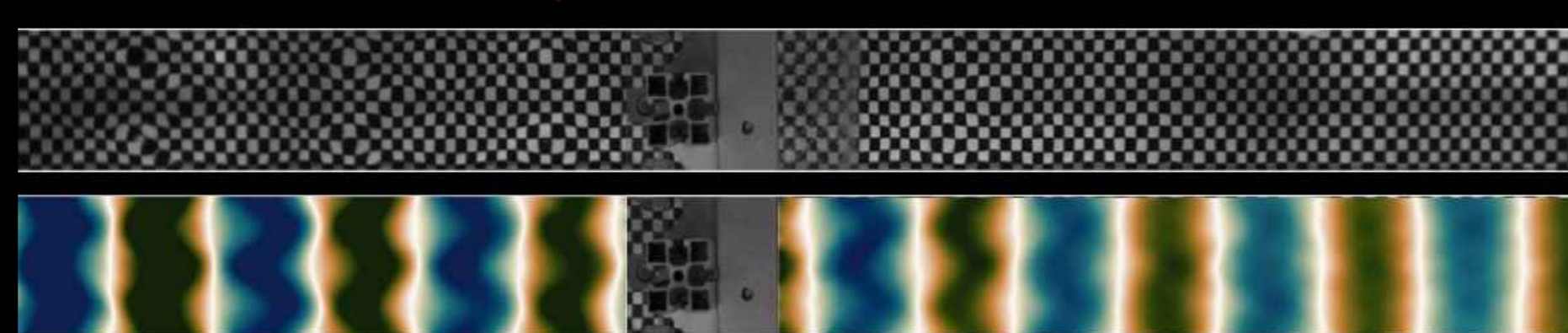
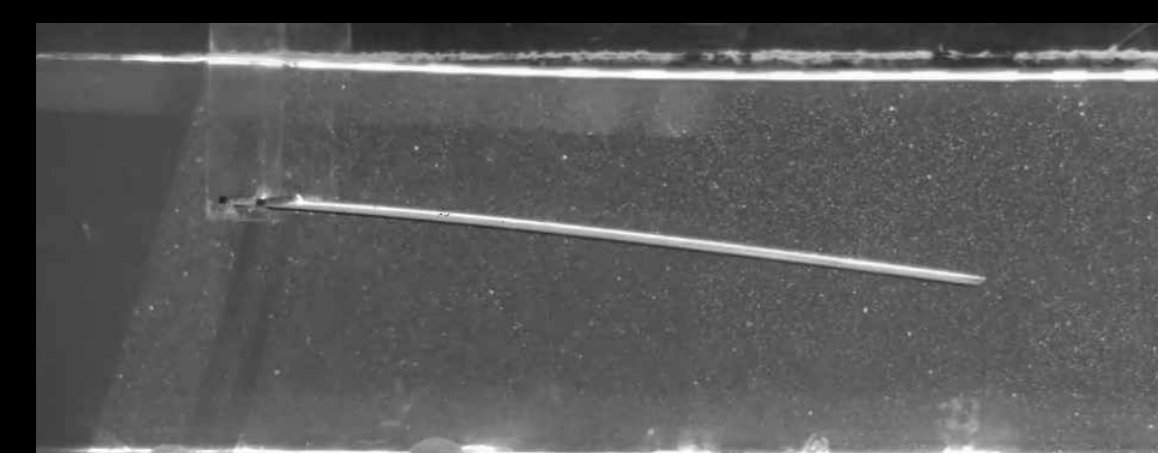


- A : wave amplitude
- T : wave period

Key wave properties such as frequency ($f = 1/T$) and amplitude can be easily varied, enabling systematic study and exploration of different regimes.



Numerical simulations can reproduce experimental configurations while offering precise control over wave conditions.



Captured using a camera via Schlieren imaging, where distortions of a checkerboard pattern are processed to reconstruct η , the free-surface elevation of the waves.



BioFSI Lab

Bioinspired Fluid-Structure Interaction Laboratory



UNIVERSITY OF BIRMINGHAM

Introduction

Corrosion fatigue crack growth is a synergistic process which leads to the failure of offshore wind support structures. Understanding the rate at which fatigue cracks grow is therefore of paramount importance.

Current recommendations on fatigue crack growth rates for structural steels in BS 7910:2019 [1], include data on the following environments: in air, submerged in seawater - unprotected free corrosion, and submerged in seawater with cathodic protection. This leaves a gap in the standard for recommendations on the splash zone. Data collected using a representative splash zone environment is not available, prompting the present investigation.

Surface corrosion tends to be more severe in the splash zone, however its effect on the fatigue crack growth rate is unknown. It may accelerate crack growth due to this increased severity, or it may blunt the crack tip for the same reason, slowing crack growth.

Experimental splash zone environment

To create realistic inputs for the splash zone test chamber, where cracked specimens will undergo fatigue loading and be exposed to a splash zone environment simultaneously, a representative sea state was generated. It was based on two input values; the significant wave height, H_s (annual mean), and the mean spring tidal range. These values were compared across five North Sea offshore wind farms; Moray West was selected as the case study site as it presented intermediate values of the sites compared [3].

A Rayleigh probability distribution was used to generate a full spectrum of wave heights from H_s . The mean wave period was estimated from H_s using the Pierson-Moskowitz spectrum, with this period assigned uniformly across all wave heights. The wave sequence was then randomised to reflect the natural irregularity of ocean waves, before the individual waves were concatenated into a continuous time series and superimposed onto the tidal range to produce a representative sea surface.

Experimental Plan

Fatigue crack growth tests were first conducted in air and fully submerged in seawater to provide a baseline. Three splash zone conditions were subsequently designed to cover a range of splash zone environments: a pre-established standard condition [2], and two conditions approximating North Sea environments. High and low load ratios were applied across all three conditions to assess load ratio sensitivity.

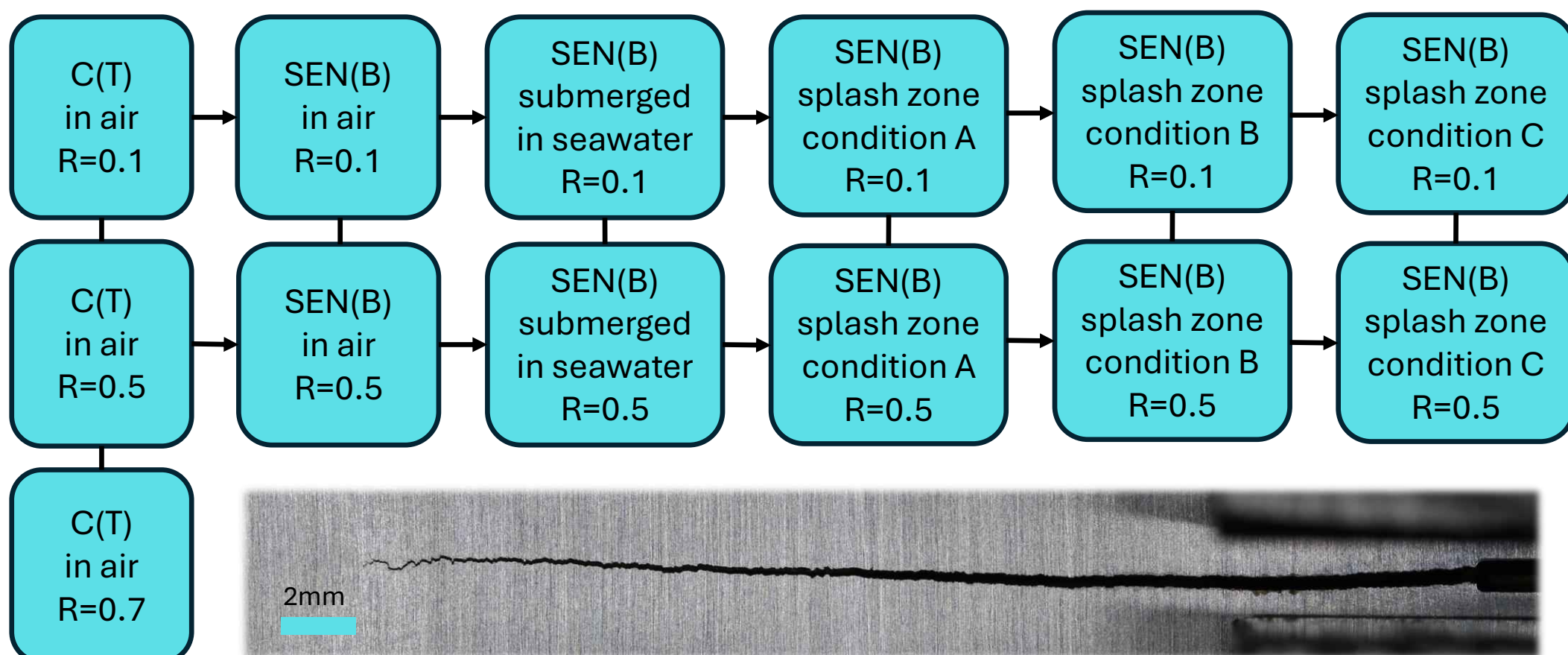


Figure 1 – Experimental plan flow chart and image from 'in air' fatigue crack growth rate test.

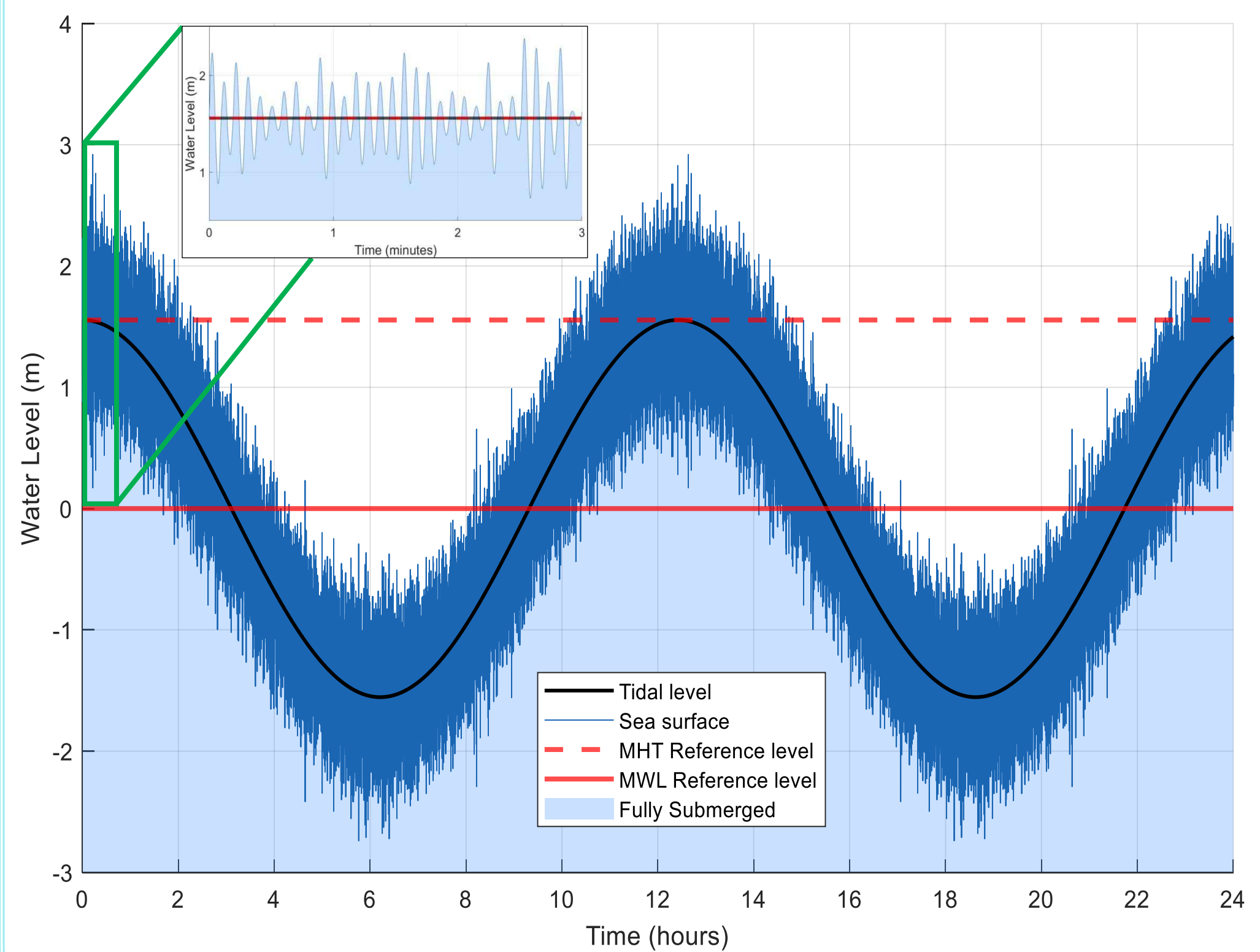


Figure 2 – Sea surface based on a mean sea state for the Moray West wind farm

Splash Zone key aspects

In the splash zone, the key corrosion characteristic which will be considered is that of cyclic wetting and drying, which is generally more aggressive than continuous immersion [4]. During drying via evaporation, an oxygen concentration gradient could develop between the crack tip and the exposed surface, driving corrosion by differential aeration. Simultaneously, the evaporation of seawater will increase the concentration of corrosive species, resulting in a highly concentrated saline solution within the crack.

Mass transport during fatigue cycling

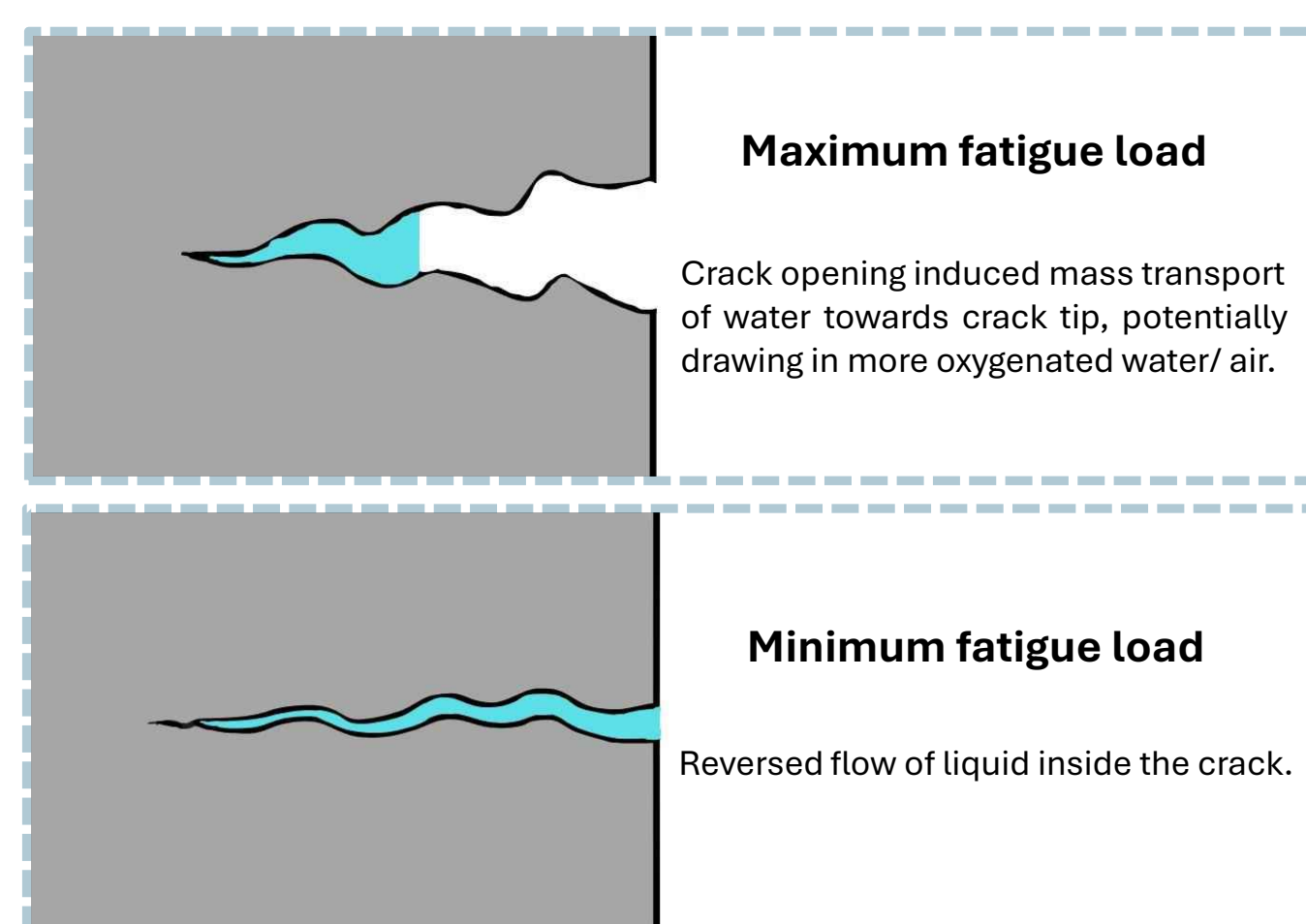


Figure 3 – Mass transport of seawater in corrosion fatigue crack.

Wet - Dry Cycling

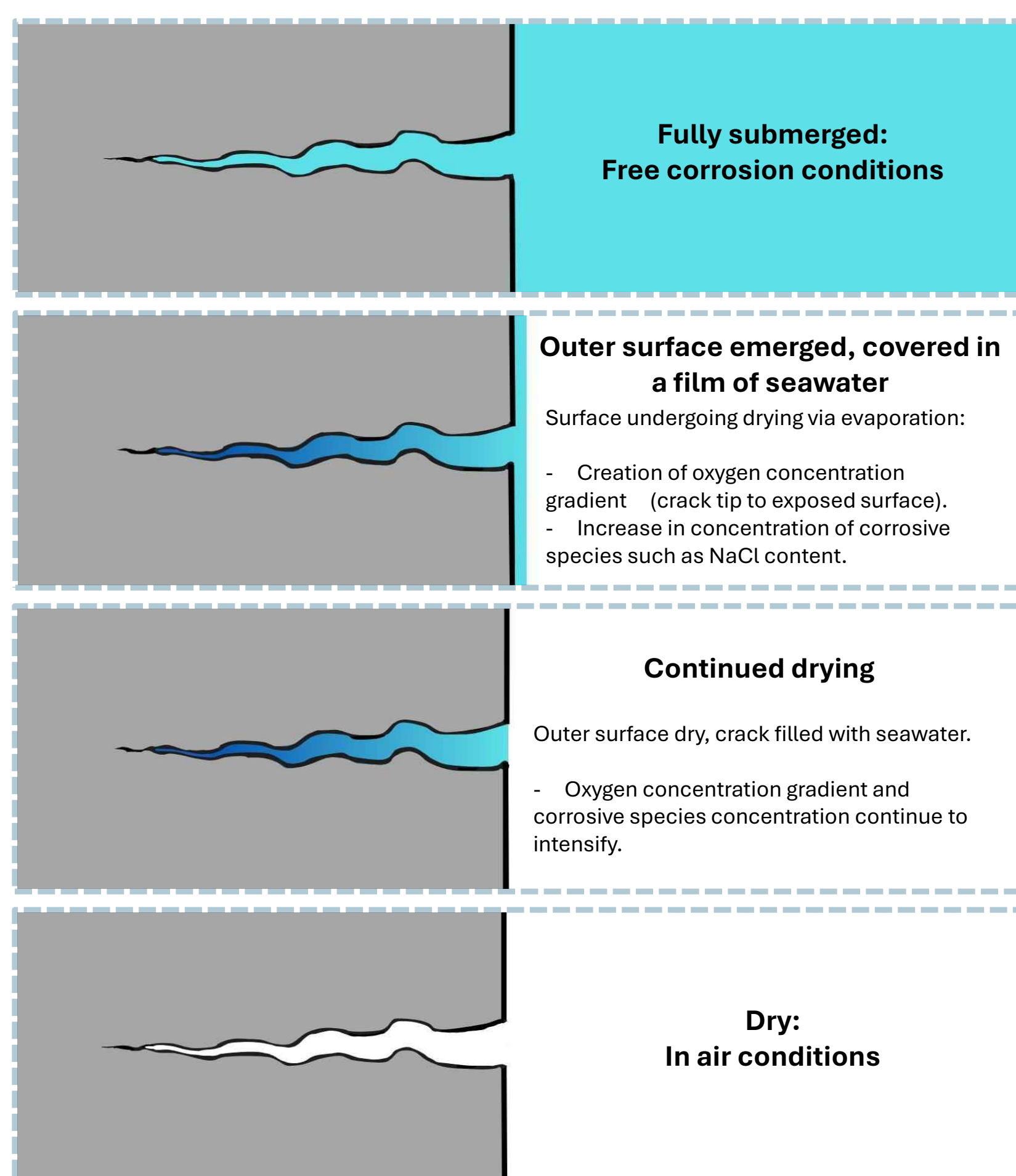


Figure 4 – Aspects of wet - dry cycling experienced by a corrosion fatigue crack.



References

1. British Standards Institution, BS 7910:2019 'Guide to methods for assessing the acceptability of flaws in metallic structures'. 2019.
2. ASTM, Standard Practice for Exposure of Metals and Alloys by Alternate Immersion in Neutral 3.5% Sodium Chloride Solution, in ASTM G44-21. 2021, ASTM International: ASTM International.
3. Marine, S. National Marine Plan Interactive (NMPI). 2024; Available from: <https://marinescotland.atkinsgeospatial.com/nmpi/default.aspx?layers=424>.
4. Genin, C., Cathodic Protection of carbon steel in the tidal zone : involved mechanisms. 2023, Université de La Rochelle.

This research is funded by TWI's Core Research Programme, a market-driven programme of research and development activities that underpin the creation and optimisation of joining, materials and engineering technologies. <https://www.twi-global.com/crp>